Macromolecules
ARTICLE

Macromolecules **2010**, *43*, 6193–6201 **6193**
DOI: 10.1021/ma100963m

Ionically Cross-Linked Triblock Copolymer Hydrogels with High Strength

Kevin J. Henderson, Tian C. Zhou, Kathryn J. Otim, and Kenneth R. Shull*

Department of Materials Science and Engineering, Northwestern University, Evanston, Illinois 60208

Received May 3, 2010; Revised Manuscript Received June 18, 2010

ABSTRACT: High strength hydrogels were made by ionically cross-linking the polyelectrolyte midblock of a self-assembled, amphiphilic triblock copolymer network. The polymer backbone consisted of glassy, spherical domains of poly(methyl methacrylate) (PMMA) end blocks bridged by solvated poly(methacrylic acid) (PMAA) midblocks, whose assembly was induced by vapor phase solvent exchange. Ionic cross-linking was achieved by submersion of polymer gels into pH-buffered solutions of divalent acetates (Zn, Ca, Ni, Co, Cu). Consequent mechanical characterization by tensile and indentation testing methods revealed a dependence of mechanical behavior on ion absorption, pH, and cation identity with orders of magnitude increases in Young's modulus between cross-linked and noncross-linked states. These materials exhibit a degree of reversible energy dissipation with mechanical responses reminiscent of tough double network hydrogels and fracture stresses up to ~1 MPa.

Introduction

Synthetic strategies for generating hydrogels that mimic the properties of tough biological materials are limited. Soft, structural materials such as cartilage exist in aqueous environments at relatively low biopolymer volume fractions while maintaining high rigidity, load bearing ability, and lubricating (low friction) properties.[1] These characteristics result from an elegant combination of protein chemistry, well-defined structure, and reversible intermolecular bonds maintained by a finely tuned, local environment. In contrast to such biological gels, conventional, chemically cross-linked polymer gels have extremely poor mechanical properties.[2−4] While conceptually similar, chemically cross-linked gels suffer from inherent network inhomogeneities, an artifact of their polymerization technique, which increases brittle character especially at higher cross-linking densities. Network homogeneity is significantly improved in triblock copolymer,[5−8] nanocomposite,[9] topological,[10] or macromolecular microsphere composite gels,[11] resulting in more robust materials capable of large strain deformation. However, the ability of these materials to undergo large strains often comes at the expense of stiffness. The ability to generate polymer gels with a large Young's modulus (~10^6 Pa) capable of large deformations is a nontrivial research feat. The most successful synthetic materials to date are double network hydrogels,[12,13] which synergistically combine the stiffness of a tightly cross-linked network with the dissipative ability of an independently formed, loosely cross-linked network. These materials have demonstrated strengths and toughnesses that rival biological cartilage.[14,15]

However, the exceptional toughness of a double network gel compromises the material's fatigue resistance, as it depends entirely upon irreversible damage to the first network as an energy dissipation mechanism. While the second network assists in broadening the fracture zone to maximize dissipation, once the first network has been fractured, the mechanical response is dominated by the much softer second network, and the high stiffness and toughness are lost. Consequently, one approach to remedy this situation is the replacement of the stiff chemically cross-linked network with one that is noncovalently, reversibly associated. The inherent problem with this solution is that reversible bonds are inevitably weak, resulting in a problematic inverse relationship between stiffness and fatigue resistance. Perhaps the best mechanism for achieving pseudocovalent bonding character, while maintaining a degree of reversibility is ionic cross-linking, which ranges in nature from mostly Coulombic attractions[16] to complicated ligand−metal complexation.[17] Judicious selection of the cross-linking ion provides a means for optimizing the overall mechanical properties of the material.

Here we employ ionic cross-linking in conjunction with a physically associated triblock copolymer network[10] to mimic the structure, and hence performance, of double network hydrogels. The polymer architecture and gel assembly process are presented in Figure 1. In contrast to true double network gels, these gels have only a single polymer network, and this network is cross-linked twice using two disparate mechanisms. The analogue of a double network gel's tightly cross-linked network is the ionically associated midblock, while the loose network analogue is the physically associated triblock copolymer backbone. The resulting hydrogels demonstrate tensile loading behavior reminiscent of double network gels but improved fatigue resistance through reversible ionic associations.

Background

Ionic Cross-Linking. Metal−carboxylate interactions between charged polyelectrolytes and divalent cations were first studied as early as the 1950s.[16,18,19] The nature of the complexation has been studied hence by a number of potentiometric,[20−24] electron paramagnetic resonance,[25,26] magnetic susceptibility,[24,25] and spectroscopic methods[19,24,27,28] for linear polyelectrolytes, cross-linked gels, and polymer brushes. These studies indicate a clear dependence of the nature of associations on the identity of the cation used. While Group II metals demonstrate a predominantly electrostatic interaction, d-block elements have the ability to complex with carboxylate ligands leading to more stable, pseudocovalent bonds with reversible character. The bond stability of complexes formed follows the Irving Williams series,[29] which fundamentally scales with decreasing cation size. However, the trend is further explained by the effect of electronic configuration through ligand field stabilization energies (LFSE) up to d^8 metals. For fourth

*Corresponding author. E-mail: k-shull@northwestern.edu.

Published on Web 07/01/2010

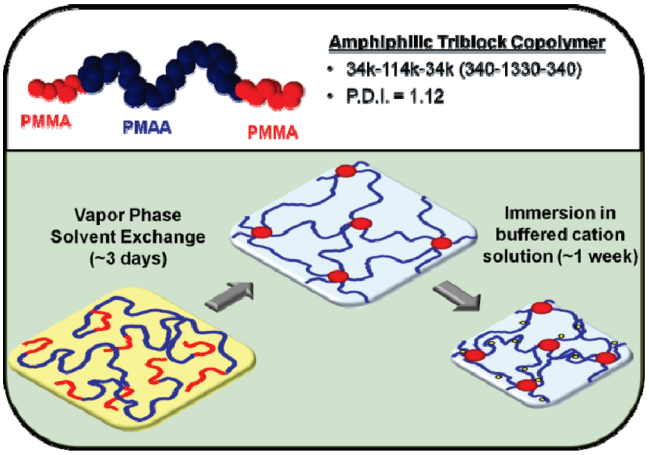

Figure 1. Structure and assembly method for obtaining ionically cross-linked hydrogels.

period elements on the periodic table, this trend follows Ca < Mn(II) < Fe(II) < Co(II) < Ni(II) < Cu(II) > Zn(II). The anomaly of Cu(II) and Zn(II), which have lower LFSE energies than Ni(II), can be attributed to complex geometry. Cu(II) complexes demonstrate tetragonal distortion of the octahedral geometry due to the Jahn−Teller effect,[30] while Zn(II) complexes are often tetrahedral rather than octahedral.[29] However, depending on the geometry adopted by Zn(II), the order of Ni(II) and Zn(II) may change and is highly ligand-dependent. The stability of metal−ligand bonds relates to the bond lifetime, with a linear relationship being quite common between the thermodynamic equilibrium constant of complex formation and the lifetime of a bond. Qualitatively, a more stable metal−ligand bond (such as with Cu(II)) will exhibit a larger bond strength and a longer bond lifetime, while a less stable bond (such as Ca) will form a weaker, more transient association. The bond association rate is fairly independent of cation identity, with the rate-determining step consisting of a dissociation of an outer sphere aqua ligand around the cation rather than bond formation with an incoming ligand.[31] However, the lifetime of these complexes after formation is dependent on the bond strength. When attached ligands are multidentate, the lifetime of formed complexes jumps dramatically since dissociation of the complex depends upon detachment of multiple bonds. Given the sensitivity of both the charged states of metallic cations and carboxylate ligands to pH, complex formation and binding modes in these experiments are highly pH dependent, with little complexation available under basic conditions due to hydroxide formation, which diminishes the polyvalent state of a hydrated cation.[32]

To date, more emphasis has been placed on characterizing the chemical nature of the metal-carboxylate interaction, while fewer studies have focused on the mechanical influence of ionic cross-linking in hydrogels. Recent work by Horkay et al.[33] suggests that divalent complexes formed with poly(acrylic acid) gels are entirely reversible, while trivalent metals are not. Furthermore, the normalized modulus of cross-linked gels increases as the strength of the carboxylate bond increases. Alginate hydrogels[34] have been studied much more extensively, though mostly in the presence of calcium cations. The mechanism of cross-linking in these systems is relatively well understood, with the calcium "egg-box" structures[35] bridging the guluronic acid moieties to produce a 3-dimensional network. The effect of ionic cross-linking in these naturally occurring biological gels is an increase in both the toughness and stiffness. Mooney et al. have recently demonstrated[36] that these alginate gels exhibit self-healing character due to the nature of the reversible calcium ionic associations.

The current study aims to elucidate the mechanical effect of ionic cross-linking on physically associated polymer hydrogels, with particular emphasis on concentration effects and pH dependence on mechanical properties as well as gel recovery following loading.

Block Copolymer Hydrogels. The acrylic block copolymer hydrogel used in this study serves as an excellent model system for a physically associated hydrogel. In contrast to a chemically cross-linked system, a physically associated hydrogel benefits from a homogeneous distribution of cross-links which enhances the large-strain deformation performance of the materials. Extensive characterization of thermoreversible, alcohol-based gels[37] similar to the triblock copolymer used in this study have elucidated the role of polymer concentration, chain composition, and block lengths on network architecture and gel performance. Small angle X-ray scattering studies and self-consistent mean-field calculations indicate that the end blocks form spherical aggregates with diameters of ∼15−20 nm. At room temperature, these aggregates are glassy and "frozen" in character, resulting in an elastic network capable of undergoing significant deformation before strain hardening, with the extent of such deformation determined by the finite extensibility of the component midblock.[38,39] These gels have Young's moduli on the order of 10^3-10^4 Pa when the polymer weight fraction is between 0.05 and 0.25 and exhibit rate-dependent toughnesses on the order of 10−100 J/m^2.[38] The copolymer used in this study demonstrates similar behavior,[40] but the thermodynamic parameters governing network structure come from the solvent composition rather than temperature. Upon solvent exchange, the resulting hydrogel can be considered equivalent to a thermoreversible gel cooled well below its gel transition temperature, such that the relaxation times of end blocks are several orders of magnitude above experimental time scales and are continually in a glassy state.

Experimental Details

Polymer Synthesis. The triblock copolymer used in this study was synthesized by anionic polymerization using a previously described technique.[40] Initially the copolymer was synthesized with a midblock of poly(*tert*-butyl methacrylate) (P*t*BMA) and PMMA end blocks. The P*t*BMA midblock length and copolymer polydispersity (PDI = 1.12) were assessed using gel-permeation chromatography (Waters 717plus autosampler connected to a Waters 2410 refractive index detector) in HPLC grade tetrahydrofuran against polystyrene standards. The end block lengths were determined using proton nuclear magnetic resonance spectroscopy (Inova 400 MHz) by comparing integrated peak ratios of the methoxy protons in PMMA (δ = 3.60 ppm) versus the *tert*-butyl protons in P*t*BMA (δ = 1.43 ppm) referenced against the measured molecular weight of P*t*BMA. In order to generate the amphiphilic copolymer, the midblock was hydrolyzed in 1,4-dioxane with a 3 times molar excess of hydrochloric acid at 80 °C for 6 h to generate a hydrophilic PMAA segment. The molecular weights of each block in the final converted polymer are 34K−114K−34K, corresponding to a degree of polymerization of 340−1330−340.

Materials. Zinc acetate, calcium acetate, cobalt acetate, nickel acetate, copper acetate, and acetic acid were purchased from Sigma-Aldrich and used as received. All buffered acetate solutions were made in nanopure water (18.2 MΩ-cm) with pH confirmed using a WTW Portable pH Tester, Model 20. Solutions of 7.0% (w/w) triblock copolymer in dimethyl sulfoxide (Aldrich) were poured into rectangular molds and stored in sealed plastic containers under saturated water vapor conditions to permit the vapor phase solvent exchange with water for 3 days,

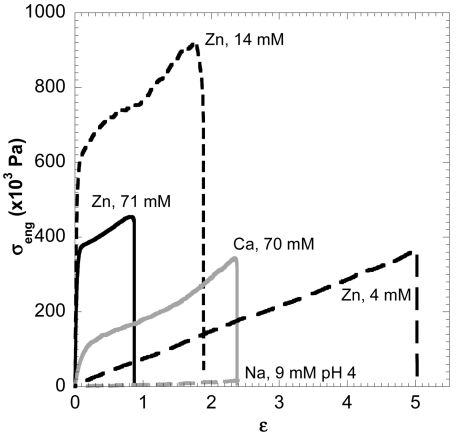

Figure 2. Stress−strain response of ionically cross-linked samples in a tensile geometry. Sample details are listed in Table 1.

during which time the increased water content induced nanophase separation of the PMMA domains into bridged, spherical aggregates. Upon solvent exchange, the polymer weight fraction was 6.0−7.0%, corresponding to an average midblock carboxylate concentration of 440−510 mM. Samples were cross-linked by subsequent immersion of gels into pH-controlled acetate solutions of divalent ions and were allowed to equilibrate for a week (gel weights and ion absorption behavior stabilize within 12−72 h for all samples) before mechanical characterization.

Methods. Tensile tests were carried out on an Instron machine with a 50 lb Sensotec load cell at a loading rate of 10 mm/min (0.5 strain/min). Dogbone samples were cut from equilibrated gel sheets with a gauge length and width of 21.0 mm and 4.2 mm, respectively. Gel thicknesses varied by salt concentrations used and ranged from 0.60 to 2.0 mm. Samples were immersed in solution until testing was carried out and were assumed to be free of significant drying during loading. Three specimens of each sample were tested, and the average modulus, fracture stress, and strain to failure reported. The samples broken at the largest strains are illustrated in Figure 2, with the strain energy density values calculated from only these specimens.

Indentation tests were carried out using an axisymmetric probe tack device, consisting of a piezoelectric stepping motor connected in parallel to a load transducer attached to a flat cylindrical indenter.[41] Displacement was monitored using an optical sensor. The cylindrical indenter used had a radius of 440 μm and was loaded at a rate of 10 μm/s. All samples were tested while immersed in buffered acetate solutions.

Ion absorption measurements were conducted using inductively coupled plasma optical emission spectroscopy on a Varian Vista MPX instrument. The emission peaks used for concentration analysis of zinc and calcium samples were 213.857 and 422.673 nm, respectively. All sample concentrations were diluted to a range of 1−40 ppm, and analyzed using a quadratic fit against prepared standards. The ion uptake within the gels was determined by the difference between the initial and final concentrations of the surrounding solution.

Results and Discussion

Tensile Behavior. Tensile tests of gel samples equilibrated for 1 week in various acetate solutions are shown in Figure 2, plotted as a function of the engineering stress, σ_{eng}, versus the engineering strain, ε. Sample details are listed in Table 1. Here, σ_{eng} is defined as the measured load divided by the undeformed cross-sectional area, and ε is defined as the extension divided by the undeformed gauge length. The polymer volume fraction for each sample is denoted by ϕ_p (assumed to equal to polymer weight fraction), and U is the strain energy density, discussed further in a subsequent section. As a control to illustrate the tensile behavior of a noncross-linked sample, the data from a sample immersed in 10 mM sodium acetate pH 4 buffer is included. The monovalent sodium ion does not coordinate with more than a single carboxylate functionality at a time and as a result does not appreciably affect mechanical properties of the bulk gel. A pH of 4 is employed here to maintain a polymer fraction similar to that of cross-linked samples ($\phi_p \sim 0.10$). The modulus of this gel is relatively small, and the gel fails at strains near 2. The material is linearly elastic, as expected at these strains. The use of a small concentration of divalent zinc (4 mM; pH 6) results in a gel with a modulus about an order of magnitude higher than the sample with no divalent salt. This sample similarly demonstrates linear elasticity as expected in the neat polymer gel but has a much larger modulus and is capable of attaining higher strains (~4−5).

A significant deviation in linear elastic behavior occurs at intermediate to high concentrations of divalent salt addition. These samples demonstrate a 2-fold loading behavior that closely resembles that of double network gels.[11] According to models developed independently by Brown[12] and Tanaka,[13] the unique loading behavior can be explained by the presence of a damage zone where a stiff network breaks above a critical stress σ_c, above which the modulus of the weaker network dominates the mechanical behavior, producing a macroscopic yielding effect. Here, a high-modulus region reminiscent of stiff ionic cross-linking is present at small strains (< 0.1), followed by an extensive high-stress region corresponding to the yielding of the ionically cross-linked network. An intermediate concentration of zinc (14 mM; pH 6) results in a deswollen gel that is considerably stiffer than gels with little or no divalent cation present. However, this increase in stiffness comes at the expense of extensibility as the sample fails near a strain of 2. Subsequent addition of zinc to a high concentration (71 mM; pH 6) results in a more swollen gel with degraded mechanical properties: a reduction in the modulus, critical stress, and strain at failure. A calcium sample at high concentration exhibits the same behavior, but has a lower modulus and can withstand slightly larger strains (~2.4). These results suggest that the extent of ionic cross-linking is highly dependent on concentration and cation identity. Low concentrations of divalent cation serve to increase both modulus and extensibility while higher concentrations begin to lose both. The cation selection governs the extent of these changes.

Concentration and pH Dependence of Modulus. The concentration dependence of the cross-linking event has been probed via indentation testing as this technique is amenable to quick testing of many small specimens. Figure 3 depicts a typical indentation loading and unloading curve, plotted as average stress (load divided by punch cross section) versus the normalized indenter displacement (displacement divided by the indenter radius). The observed Young's modulus is defined by the following equation:[42,43]

$$E = \frac{3\pi\sigma_{av}}{8(\delta/a)} \quad (1)$$

Here σ_{av} is the average stress under the indenter, δ is the indenter displacement, and a is the indenter radius. The sample thicknesses are all at least 4 times the punch radius, so the effect of confinement on the modulus measured by indentation does not need to be taken into account.[44] In these experiments, we obtain an effective modulus, E_{eff}, at intermediate values of the normalized displacement (~0.2) where the gel's mechanical response is still linearly elastic and artifacts of initial loading behavior (e.g., uneven surface) are not evident. We refer to the modulus obtained from

Table 1. Sample Information for the Specimens from Figure 2[a]

ion, c_{out}	ϕ_p	E (MPa)	fracture stress (MPa)	strain at fracture	U (MJ/m^3)
Zn, 4 mM	0.29	0.075 ± 0.001	0.30 ± 0.06	4.2 ± 0.8	0.98
Zn, 14 mM	0.40	21 ± 4	0.86 ± 0.09	1.7 ± 0.3	1.4
Zn, 71 mM	0.18	10 ± 1	0.44 ± 0.02	0.78 ± 0.11	0.32
Ca 70 mM[b]	0.48	1.0 ± 0.1	0.30 ± 0.03	2.4 ± 0.1	0.24
Na, 9 mM pH 4[b]	0.10	0.0046 ± 0.0006	0.011 ± 0.005	2.0 ± 0.38	0.02

[a] The Young's modulus, fracture stress, and strain at fracture values are averaged from three specimens, while the values of the strain energy density, U, come from the samples with the largest strain at fracture. Errors reflect 1 standard deviation from the average. [b] Denotes an estimated concentration relative to measured quantities.

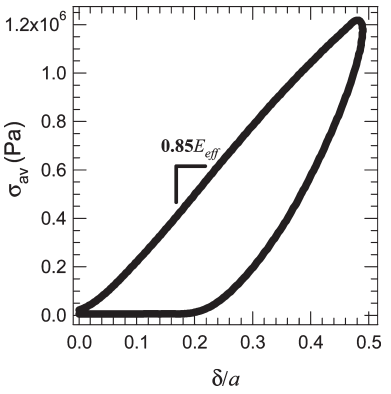

Figure 3. Typical indentation loading and unloading curve illustrating the determination of the effective modulus for a zinc sample (C_{out} = 92 mM; pH 6).

application of eq 1 to the indentation data as an effective modulus due to the discrepancy between moduli obtained from indentation and tensile methods for stiff, cross-linked samples. The indentation tests, which result in localized stresses above the yield stresses observed under tension, can lead to localized gel failure and result in an observed softening in the modulus. This phenomenon is attributed to the inhomogeneous stress state beneath the flat punch which possesses a singularity at the punch edge.[14]

Figure 4 illustrates the effect of ionic identity and concentration on Young's modulus as determined from the indentation experiments. External concentrations (c_{out}) indicated in these plots are the actual final concentrations of the solutions that are in equilibrium with the gels. Because of the observed softening of ionically cross-linked samples in the indentation geometry, these effective moduli serve as a lower bound for the actual, low-strain moduli. The tensile data from Figure 2 provide a better quantitative measure of sample stiffness, and these values indicate that difference between E and E_{eff} is larger for the highly cross-linked Zn samples ($E/E_{\mathrm{eff}} \sim 6$) than for the highly cross-linked Ca samples ($E/E_{\mathrm{eff}} \sim 3$). From Figure 4, it is readily apparent that monovalent cations such as sodium have little effect on the modulus across all concentrations, whereas the divalent cations calcium and zinc lead to an increase in the modulus by orders of magnitude. At low concentrations, all samples exhibit similar moduli, and at higher concentrations the divalent cation samples exhibit an abrupt transition from a low-modulus to a high-modulus state, indicative of saturated ionic cross-linking. With zinc, this transition occurs near a 4 mM concentration, while the transition for calcium is closer to 16 mM, four times higher. Furthermore, the fully cross-linked moduli for zinc samples are an order of magnitude higher than calcium, consistent with the tensile testing results. Upon obtaining a cross-linked state for both divalent ions, the effective modulus reaches a peak and weakly decreases as concentration increases, remaining on the same order of magnitude. This decrease can be attributed to a change in polymer fraction, which will be discussed subsequently. A decrease in solution pH from pH 6 to pH 4 only serves to change the concentration necessary to achieve cross-linking but does not entirely prevent cross-linking from occurring.

Ion Absorption Measurements. Ion absorption experiments were conducted to determine the final equilibrium concentrations of ions in the prepared gels and also served to quantify the ion uptake into the gels which contributed to the observed mechanical properties. Figure 5 shows the relationship between the interior and exterior ion concentrations (c_{in} and c_{out}) for zinc and calcium cross-linked gels. The internal concentration of the gel assumes a density of 1.0 g/cm^3, using the gel weight as a measure of volume.

The results indicate that the ion concentration within the gel is consistently larger by an order of magnitude or more in comparison to the ion concentration outside the gel, which can readily be explained by the affinity of the negatively charged polymer backbone for the positively charged counterions. For both cations at pH 6, there is a considerable spike in ionic uptake that coincides with a transition in volume and modulus, with this transition occurring earlier for Zn than Ca. Above these spikes at higher relative values of c_{out}, the c_{in} concentrations of both Zn and Ca are roughly the same. The preferential absorption of cations by the gel begins to taper off at high concentrations as the network becomes saturated with ions. For the pH 4 samples, there is no clear distinction between Ca and Zn samples, with both following a linear trend at low concentrations and showing a slight spike at high concentrations similar to the pH 6 samples where an increase in mechanical stiffness becomes prevalent.

Figure 6 is a plot of the same data in reference to the fractional uptake of cations absorbed by the gel. Here we calculate this ratio (f_{Zn} or f_{Ca}) using the following equation:

$$f_{ion} = \frac{(c_{in} - c_{out})}{c_{COOH}} \qquad (2)$$

Here c_{COOH} is the molar concentration of the midblock monomer within the gel. This equation discounts free ions in solution within the gel and assesses only the bound cations. For 100% association between the divalent cations and the carboxylates, f_{ion} would be 0.5. At a pH of 6, this limit is approached for both the Zn and Ca ions at sufficiently high external ion concentrations, although the absorption ratios for both cations are lower at pH = 4. Furthermore, it is evident that cation identity yields little influence on f_{ion} with all pH 6 and pH 4 samples virtually indistinguishable between the two cations studied.

Figure 6b illustrates that while f_{ion} is virtually equivalent across all concentrations for both cations, the swelling states (as denoted by polymer volume fraction, ϕ_p) are quite distinguishable. Zn samples exhibit a volume transition at lower values of f_{ion} than Ca samples and also swell out to lower values of ϕ_p upon saturation. This difference in

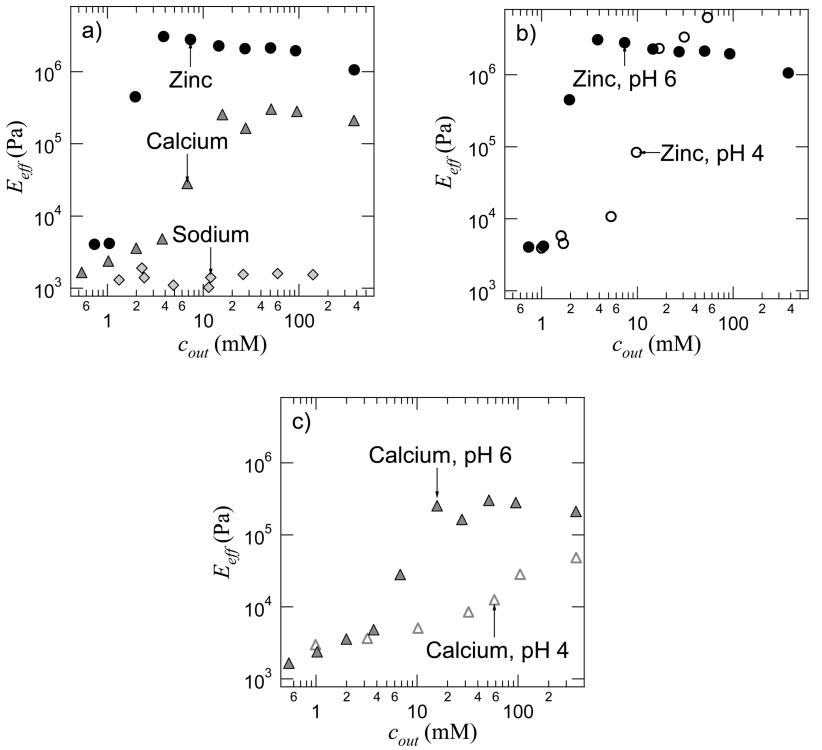

Figure 4. (a) Concentration dependence on Young's modulus, E_{eff}, for sodium (diamond), calcium (triangle), and zinc (circle) cross-linked samples at pH 6. (b) Young's modulus of zinc cross-linked samples at pH 4 (open) and 6 (closed) and (c) Young's modulus of calcium cross-linked samples at pH 4 (open) and 6 (closed).

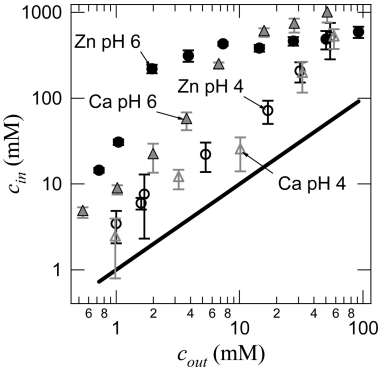

Figure 5. Cation concentration in the gel versus exterior solution concentration. Calcium samples are represented by triangles while zinc samples are circles, and pH 6 samples are closed symbols while pH 4 samples are open. The black line represents an ideal 1:1 relationship between interior and exterior concentration when no favorable interactions exist between ions and the polymer within the gel. Error bars indicate ±1 standard deviation.

swelling originates from the nature of the detailed cross-linking mechanism, perhaps related to the different geometries of the complexes that are formed. Regardless of the mechanism, it is clear that the polymer volume fraction is not merely dependent upon the fraction of absorbed cations with the gel.

Relationship between Modulus and Polymer Concentration. Given the differences in swelling behavior for each cation, it is necessary to take into account this variable to develop a better understanding of cross-linking behavior. To demonstrate the role of polymer fraction in the observed mechanical response of samples, the combined data for all indentation measurements are shown in Figure 7 as a function of ϕ_p. At low ion concentrations the modulus increases as ${\phi_p}^{1/3}$, consistent with a material that obeys the following expression obtained from a standard neo-Hookean model of rubber elasticity:[45]

$$E = \frac{3\beta{\phi_p}^{1/3}\rho RT}{M} \tag{3}$$

Here, M is the average molecular weight between cross-link points, which for the un-cross-linked polymer is simply the total copolymer molecular weight (182 kg/mol), and ρ is the polymer density. We have assumed here that the fraction of midblocks that bridge different PMMA end block domains is equal to one, which has previously been shown to be a good approximation for triblock gels with these concentrations and molecular weights.[46] The quantity β is the ratio of the root-mean-square end-to-end distance of the polymer in the collapsed, dry state normalized by the value it would have in a Gaussian polymer melt. A value of 0.24 for β describes the behavior of the noncross-linked polymers. At low ion concentrations, the effect of the ions is merely to deswell the network, thereby increasing ϕ_p. Intermolecular cross-linking that would result in a higher elastic modulus is not observed under these conditions.

At higher concentrations of divalent salts, the modulus begins to deviate significantly from the form of eq 3 that is valid at low ion concentrations, providing a clear signature of ionic cross-linking. Once the modulus has peaked for a given cation, the modulus once again scales with polymer fraction as increasing concentration leads to reswelling of the polymer network and an accompanying decrease in modulus. This phenomenon suggests that ionic cross-links become saturated, and the molecular weight between cross-links remains constant despite additional increases in concentration. For the Zn cross-linked system we can fit the modulus data with eq 3, obtaining a reduction in M from 182 kg/mol to 0.52 kg/mol between cross-linked and un-cross-linked states. This value for M corresponds to an average of 6 methacrylic

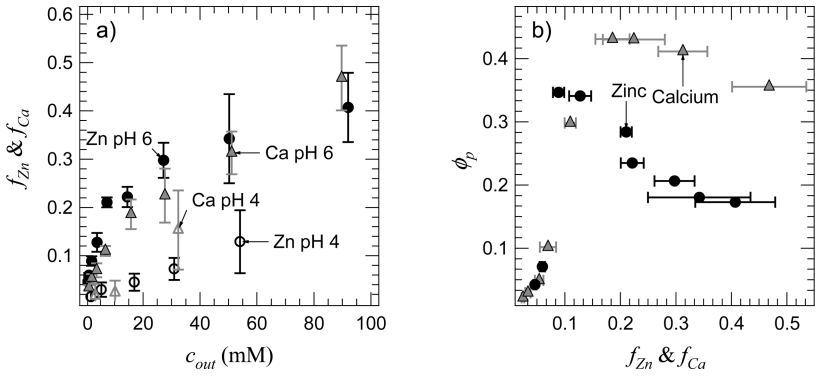

Figure 6. Plots showing (a) cation absorption in the gel as defined by the ratio of the absorbed cation concentration to the internal carboxylate concentration plotted against the equilibrium external concentration of cation and (b) gel polymer volume fraction plotted against the same ratio. Calcium samples are represented by triangles while zinc samples are circles, and pH 6 samples are closed symbols while pH 4 samples are open. Error bars indicate ±1 standard deviation.

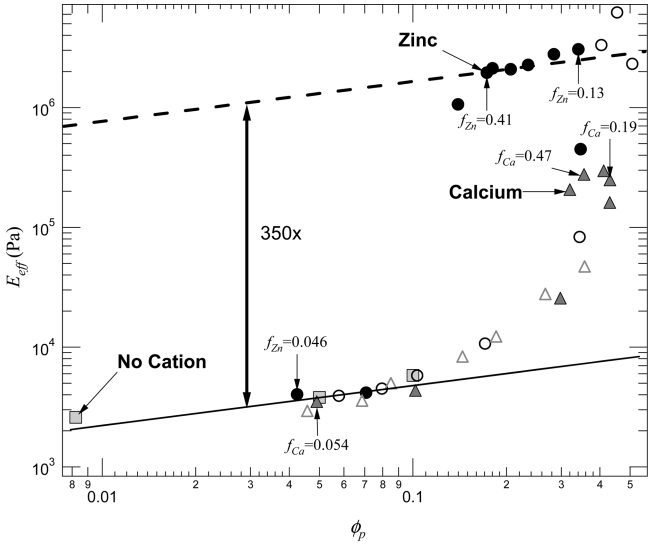

Figure 7. Indentation testing results plotting the Young's modulus of ionically cross-linked samples as a function of polymer fraction. Zinc samples are shown as circles, calcium samples are shown as triangles, and noncross-linked samples are shown as squares, with pH 6 samples shown as filled symbols and pH 4 samples shown as open symbols. The lines correspond to eq 3 with $\beta = 0.24$ and $M = 182$ kg/mol (un-cross-linked state − solid line) and $M = 520$ g/mol (fully cross-linked state − dashed line).

acid groups between ionic cross-links. As a reminder, the moduli obtained from the indentation measurements are lower bounds as a result of sample yielding caused by the indentation geometry, with the softening accounting for roughly a 6× decrease in the observed modulus. Accounting for this difference results in a calculated average of 1 methacrylic acid group between cross-links, or a completely associated system. However, the use of Gaussian chain statistics to describe the elastic properties are clearly problematic for these very highly cross-linked systems. Experimental comparison to the measured value of f_{ion} at the signature cross-linking transition for each cation (~0.15) results in calculated average distances of about 3 methacrylic acid units per cross-link.

In order to illustrate the degree of cross-linking that is necessary to affect the mechanical properties of the gels substantially, we show several key values of f_{Ca} and f_{Zn} in Figure 7. The first of these are relatively low values (f_{Zn} = 0.046 and f_{ca} = 0.054), where the ions deswell the gel but do not have any effect on the average molecular weight between cross-links. Next, we show values corresponding to the maximum value of the effective modulus, corresponding also to the point of maximum deswelling. Values for f_{Zn} and f_{Ca} at this point are both close to 0.15. Further addition of cations to the gel does not increase the effective molecular weight between cross-links and results in a reswelling of the gel to give smaller polymer volume fractions.

Effect of Cation Identity on Bond Strength. Our interpretation of the difference between the maximum effective moduli obtained with Zn and Ca ions is that cross-links obtained with Zn are much stronger than those obtained with Ca. It is most accurate to view these bonds as having lifetimes that depend on the applied force.[47] A given applied stress will relax more quickly when applied to the Ca cross-linked system than when applied to the Zn cross-linked system. Equivalently, maximum stress that can be supported by the Ca cross-linked system over a specified time period will be less than the stress that can be applied to the Zn cross-linked system. As the applied stress is increased in order to measure the modulus of stiffer samples with the indentation test, the samples start to yield, giving modulus values that depend on the actual strength of the ionic cross-links. As a result, we obtain lower values of the effective modulus for the Ca-cross-linked samples than we obtain from the Zn-cross-linked samples.

Differences in bond strengths for Ca- and Zn-cross-linked systems can be attributed to the fact that group II metals, such as calcium, are considered to have only electrostatic interactions with charged polyelectrolytes, while transition metals adopt more complicated interactions according to the electronic state of the cations' d-orbital configuration. Here, we demonstrate the effect of this relationship through a series of samples made from the same initial concentration and tested using the indentation geometry. All samples were made at pH 6 and were equilibrated with external ion concentrations of 100 mM, high enough in all cases to reach the fully cross-linked state (represented by the dashed line in Figure 7 for the Zn-cross-linked system). Since these concentrations are well above the requisite concentrations needed to achieve cross-linking, the final cross-linked states can be normalized by polymer fraction to compare stiffening quantitatively. The results are shown in Figure 8. For these samples, the stiffness values coincide with the predicted behavior of the Irving−Williams series, with Ca < Co < Ni < Zn < Cu. In addition, the results indicate that all the transition metal ions enhance stiffness significantly more than calcium. Since the metal−carboxylate bond stability follows this same sequence, there exists a clear relationship between the bond stability and enhancement in stiffness caused by ionic cross-linking.

Comparison to Covalently Cross-Linked Double Network Gels. While indentation tests lucidly define the cross-linking state across a number of variables, they do not directly measure the toughness of these samples. Fortunately, recent tensile measurements of double network gels provide a standard of comparison to the experiments performed in Figure 2, and these materials have fracture toughnesses that have been well-documented.[48] To make this comparison, we use the model developed by Brown[49] and Tanaka[50] that assumes a relationship between the size of the fracture zone, h_f, and the fracture toughnesses in these materials through the following relationship:

$$G_C \approx U h_f \tag{4}$$

where U is the strain energy density of the material (J/m^3) and G_c is the fracture toughness. For double network gels, measured h_f values range from 150 to 700 μm depending on the tearing velocity studied.[51] Assuming that h_f is similar between both types of materials, the fracture toughness scales directly with the value of U in each material. For double network gels, this value is between 0.91- 5.25 $\times$ 10^6 J/m^3, depending on how the value is assessed.[51] We obtain the value of U in our gels by using the integrated area under the stress strain curve:

$$U = \int \sigma \, d\lambda \tag{5}$$

The values of strain energy density are shown in Table 1. Here we use only the samples that failed at the highest strains in our calculation to more closely match the theoretical value obtained upon loading to the critical onset strain for strain hardening, employed by Yu et al.[51]For the stiffer zinc samples, these values fall between 0.32 and 1.4 $\times$ 10^6 J/m^3, while calcium samples are slightly lower with 0.23−0.47 $\times$ 10^6 J/m^3. These values are smaller than the best double network gels, but it should be noted that calculated value of U is highly dependent on the strain onset of gel failure. In the double network calculations, U is defined as the integrated stress−strain area up to the onset of strain hardening, while many tensile loaded samples fail at much lower strains (2−3 times) due to loading rate and inherent sample imperfections. Here, we do not reach the onset of strain hardening, which is anticipated to be larger than 5 as supported by the 4 mM Zn sample. As a result, differences between these gels and double network gels are within measurable uncertainty. Regardless, these gels demonstrate 1−2 orders of magnitude improvement in U over nonionically cross-linked samples (0.02 $\times$ 10^6 J/m^3). Assuming that G_c also scales with U for triblock copolymer gels. These results suggest that ionically cross-linked gels have toughness values that fall between 100 and 1000 J/m^2, since similar triblock copolymer gels demonstrate velocity-dependent fracture toughnesses[38] between 10 and 100 J/m^2. This estimation is further corroborated by indirect comparison with the strain energy densities of double network gels.

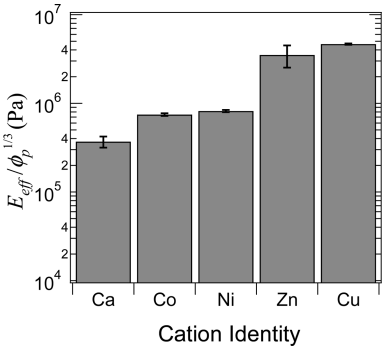

Figure 8. Plot of the normalized modulus ($E/\phi_p^{1/3}$) for a number of divalent cations at an initial concentration of 100 mM. Error bars indicate ±1 standard deviation.

A direct comparison can be made for the strengths of these ionically cross-linked materials versus double network gels. Double network gels demonstrate strengths in the range of 1−10 MPa, with a clear dependence of this strength on the cross-linking density of the second network.[12] The fracture stresses depicted in Table 1 for the ionically cross-linked specimens are clearly on the lower end of this range (0.3−0.9 MPa) but are still remarkably large in comparison to most polymer gels, particularly nonchemically cross-linked ones. For instance, gelatin, agarose, and alginate gels fail below 100 kPa of tensile stress[52,53] while the nonionically cross-linked sodium acetate samples listed in Table 1 fail near 11 kPa. The extension of ionic cross-linking to the physically associated triblock copolymer network clearly results in gels with 1−2 orders of magnitude increase in mechanical strength.

Evidence of Fatigue Resistance. The distinct advantage these materials have over traditional, covalently cross-linked double network gels is their potential self-healing ability since double network gels have no fatigue resistance. Ionic cross-linking in alginate gels has previously demonstrated reversible associations that permit gel recovery after failure in shear,[18] but similar tests have not been demonstrated in other hydrogel systems at higher ionic concentrations. Here, repeated indentation loadings of ionically cross-linked samples reveal their ability to dissipate energy reversibly, important for sustained use of these materials for any mechanical function. Parts a and b of Figure 9 depict repeated loadings for zinc and calcium gels equilibrated at pH 6 at concentrations just above the cross-linking thresholds for each cation

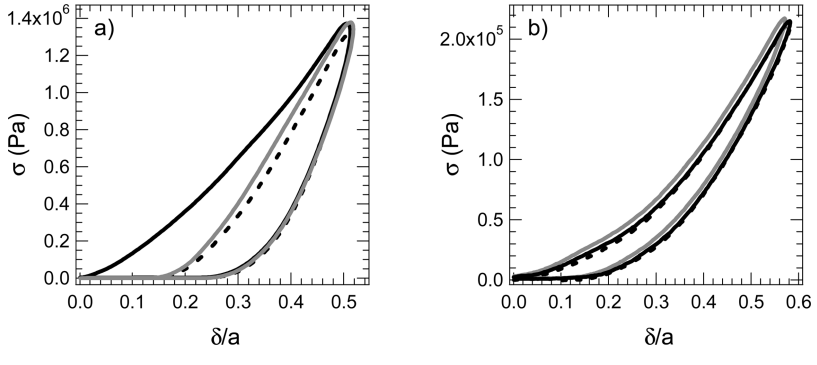

Figure 9. Repeated indentation tests of (a) zinc acetate (C_{out} = 7.3 mM; pH 6) and (b) calcium acetate (C_{out} = 27 mM; pH 6) samples. Samples were initially loaded (solid black) followed by an immediate second loading (dashed black) and a third loading after 12 h (solid gray).

(7.3 mM Zn, f_{Zn} = 0.21; 27 mM Ca, f_{Ca} = 0.22). For a nonionically cross-linked hydrogel, the mechanical response is dominated entirely by an elastic, recoverable response, with little hysteresis indicative of energy dissipation upon loading. These samples can be reloaded multiple times in a single location with almost no change in the loading/unloading behavior. In contrast, zinc-cross-linked gels (Figure 9a) demonstrate considerable hysteresis, indicating significant dissipation of applied stresses. For a sample with no fatigue resistance, a second loading in the same location would follow the unloading behavior of the previous test, a phenomenon commonly witnessed with double network gels.[54] However, upon an immediate subsequent reloading in this case, a degree of fatigue resistance is evident, with 50% of the original dissipation recovered. Upon waiting 12 h to load a third time in the same location, the recovered energy dissipated is 61% of the original dissipation, reminiscent of a self-healing mechanism. For calcium samples, the dissipation is much more recoverable, with virtually no statistically significant difference in the integrated intensities between the three loading curves. The difference in recoverability is believed to scale once again with bond stability. The less stable calcium bonds are entirely reversible on these time scales because of the shorter bond lifetimes. The zinc bonds recover less significantly and more slowly. From this behavior, it follows that increased fatigue resistance comes at the expense of network rigidity, a balance that can be tuned as desired by choosing from a range of cross-linking ions.

Conclusions

Here we have presented the ability to ionically cross-link physically associated hydrogels for enhancing mechanical performance. The results can be summarized as follows:

- Ionic cross-linking is concentration dependent, with stiffnesses of the fully cross-linked gels being up to several hundred times larger than the stiffnesses of the noncross-linked gels.
- Bond stability determines the strength of cross-links, with more permanent associations leading to stiffer hydrogels. Ionic cross-links with weaker bonds are less stiff, but more likely demonstrate the sort of recoverable energy dissipation that is necessary for fatigue resistance.
- Bond strength increases with cation identity according to the following sequence: Ca < Co(II) < Ni(II) < Zn(II) < Cu(II).
- The pH of the sample shifts the requisite concentration required for cross-linking but does not affect the final cross-linked state. The pH influences the associative ability of polymer midblock carboxylates by changing the availability of deprotonated, charged monomer units.
- The tensile loading behavior of ionically cross-linked gels is similar to that of covalently cross-linked double network hydrogels, with initial stiffnesses of several megapascals, and ultimate fracture strengths in the megapascal range. Much of the energy dissipation is recoverable, and the ionically cross-linked materials are expected to demonstrate excellent fatigue resistance in addition to high toughness upon subsequent testing.

Acknowledgment. This material is based on work supported under a National Science Foundation Graduate Research Fellowship and supported through the NSF MRSEC program (DMR-0520513) at the Northwestern University Materials Research Science and Engineering Center. ICP-AES (NSF-funded) and NMR (Pfizer donation) instruments were used in the Integrated Molecular Structure Education and Research Center (IMSERC) at NU.

References and Notes

(1) Fung, Y. *Biomechanics: Mechanical Properties of Living Tissue*, 2nd ed.; Springer-Verlag, Inc.: New York, 1981.
(2) Bonn, D.; Kellay, H.; Prochnow, M.; Ben-Djemiaa, K.; Meunier, J. *Science* **1998**, *280*, 265.
(3) Tanaka, Y.; Fukao, K.; Miyamoto, Y. *Eur. Phys. J. E* **2000**, *3*, 395.
(4) Zarzycki, J. *J. Non-Cryst. Solids* **1988**, *100*, 359.
(5) Brown, W.; Schillen, K.; Almgren, M.; Hvidt, S.; Bahadur, P. *J. Phys. Chem.* **1991**, *95*, 1850.
(6) Sato, T.; Watanabe, H.; Osaki, K. *Macromolecules* **2000**, *33*, 1686.
(7) Laurer, J. H.; Mulling, J. F.; Khan, S. A.; Spontak, R. J.; Bukovnik, R. *J. Polym. Sci., Part B: Polym. Phys.* **1998**, *36*, 2379.
(8) Soenen, H.; Berghmans, H.; Winter, H. H.; Overbergh, N. *Polymer* **1997**, *38*, 5653.
(9) Haraguchi, K.; Takehisa, T. *Adv. Mater.* **2002**, *14*, 1120.
(10) Okumura, Y.; Ito, K. *Adv. Mater.* **2001**, *13*, 485.
(11) Huang, T.; Xu, H. G.; Jiao, K. X.; Zhu, L. P.; Brown, H. R.; Wang, H. L. *Adv. Mater.* **2007**, *19*, 1622.
(12) Gong, J. P.; Katsuyama, Y.; Kurokawa, T.; Osada, Y. *Adv. Mater.* **2003**, *15*, 1155.
(13) Gong, J. P. *Soft Matter* **2010**, *6*, 2583.
(14) Kerin, A. J.; Wisnom, M. R.; Adams, M. A. *Proc. Inst. Mech. Eng. Part H-J. Eng. Med.* **1998**, *212*, 273.
(15) ChinPurcell, M. V.; Lewis, J. L. *J. Biomech. Eng.-Trans. ASME* **1996**, *118*, 545.
(16) Wall, F. T.; Drenan, J. W. *J. Polym. Sci.* **1951**, *7*, 83.
(17) Wall, F. T.; Gill, S. J. *J. Polym. Phys. A* **1954**, *58*, 1128.
(18) Gregor, H. P.; Luttinger, L. B.; Loebl, E. M. *J. Phys. Chem.* **1955**, *59*, 34.
(19) Kotliar, A. M.; Morawetz, H. *J. Am. Chem. Soc.* **1955**, *77*, 3692.
(20) Porasso, R. D.; Benegas, J. C.; van den Hoop, M. A. G. T. *J. Phys. Chem. B* **1999**, *103*, 2361.
(21) Gustafson, R. L.; Lirio, J. A. *J. Phys. Chem.* **1968**, *72*, 1502.
(22) Roma-Luciouw, R.; Sarraf, L.; Morcellet, M. *Eur. Polym. J.* **2001**, *37*, 1741.
(23) Morlay, C.; Mouginot, Y.; Cromer, M.; Chuatelut, M.; Vittori, O. *Can. J. Chem.* **2000**, *78*, 1637.
(24) Anspach, W. M.; Marinsky, J. A. *J. Phys. Chem.* **1975**, *79*, 433.
(25) Yokoi, H.; Kawata, S.; Iwaizumi, M. *J. Am. Chem. Soc.* **1986**, *108*, 3361.
(26) Varghese, S.; Lele, A. K.; Srinivas, D.; Mashelkar, R. A. *J. Phys. Chem. B* **2001**, *105*, 5368.
(27) Konradi, R.; Ruhe, J. *Macromolecules* **2004**, *37*, 6954.
(28) Linden, L. A.; Rabek, J. F. *J. Appl. Polym. Sci.* **2003**, *50*, 1331.
(29) Shriver, D.; Atkins, P. *Inorganic Chemistry*, 3rd ed.; W. H. Freeman and Company: New York, 1999.
(30) Englman, R. *The Jahn-Teller effect in molecules and crystals*; Wiley: London, 1972.
(31) Cotton, F. A.; Wilkinson, G. W. *Advanced Inorganic Chemistry*, 3rd ed.; Interscience: New York, 1972.
(32) Habert, A. C.; Huang, R. Y. M.; Burns, C. M. *J. Appl. Polym. Sci.* **1979**, *24*, 489.
(33) Horkay, F.; Tasaki, I.; Basser, P. J. *Biomacromolecules* **2001**, *2*, 195.
(34) Kong, H. J.; Wong, E.; Mooney, D. J. *Macromolecules* **2003**, *36*, 4582.
(35) Grant, G. T.; Morris, E. R.; Rees, D. A.; Smith, P. J. C.; Thom, D. *FEBS Lett.* **1973**, *32*, 195.
(36) Park, H.; Kang, S. W.; Kim, B. S.; Mooney, D. J.; Lee, K. Y. *Macromol. Biosci.* **2009**, *9*, 895.
(37) Seitz, M. E.; Burghardt, W. R.; Faber, K. T.; Shull, K. R. *Macromolecules* **2007**, *40*, 1218.
(38) Seitz, M. E.; Martina, D.; Baumberger, T.; Krishnan, V. R.; Hui, C. Y.; Shull, K. R. *Soft Matter* **2009**, *5*, 447.
(39) Erk, K. A.; Henderson, K. J.; Shull, K. R. *Biomacromolecules* **2010**, *11*, 1358.
(40) Guvendiren, M.; Shull, K. R. *Soft Matter* **2007**, *3*, 619.
(41) Webber, R. E.; Shull, K. R. *Macromolecules* **2004**, *37*, 6153.
(42) Sneddon, I. N. *Int. J. Eng. Sci.* **1965**, *3*, 47.
(43) Johnson, K. *Contact Mechanics*; Cambridge University Press: Cambridge, U.K., 1985.
(44) Shull, K. R. *Mater. Sci. Eng. R-Rep.* **2002**, *36*, 1.
(45) Flory, P. J.; Rehner, J. *J. Chem. Phys.* **1943**, *11*, 512.
(46) Bras, R. E.; Shull, K. R. *Macromolecules* **2009**, *42*, 8513.
(47) Evans, E.; Ritchie, K. *Biophys. J.* **1997**, *72*, 1541.

(48) Tanaka, Y.; Kuwabara, R.; Na, Y. H.; Kurokawa, T.; Gong, J. P.; Osada, Y. *J. Phys. Chem. B* **2005**, *109*, 11559.
(49) Brown, H. R. *Macromolecules* **2007**, *40*, 3815.
(50) Tanaka, Y. *Epl* **2007**, *78*, 5.
(51) Yu, Q. M.; Tanaka, Y.; Furukawa, H.; Kurokawa, T.; Gong, J. P. *Macromolecules* **2009**, *42*, 3852.
(52) Drury, J. L.; Dennis, R. G.; Mooney, D. J. *Biomaterials* **2004**, *25*, 3187.
(53) Mcevoy, H.; Rossmurphy, S. B.; Clark, A. H. *Polymer* **1985**, *26*, 1493.
(54) Webber, R. E.; Creton, C.; Brown, H. R.; Gong, J. P. *Macromolecules* **2007**, *40*, 2919.